



Earthquakes from a radiological perspective: what is demanded from the radiologists, and what can we do? A pictorial review

Sonay Aydin¹
 Omer Kazci²
 Bunyamin Ece³
 Mecit Kantarci¹

¹Erzincan Binali Yıldırım University Faculty of Medicine, Department of Radiology, Erzincan, Turkey

²Ankara Training and Research Hospital, Clinic of Radiology, Ankara, Turkey

³Kastamonu University Faculty of Medicine, Department of Radiology, Kastamonu, Turkey

ABSTRACT

Earthquakes are among the most destructive and unpredictable natural disasters. Various diseases and ailments, such as bone fractures, organ and soft-tissue injuries, cardiovascular diseases, lung diseases, and infectious diseases, can develop in the aftermath of severe earthquakes. Digital radiography, ultrasound, computed tomography, and magnetic resonance imaging are significant imaging modalities utilized for the quick and reliable assessment of earthquake-related ailments to facilitate the planning of suitable therapy. This article examines the usual radiological imaging characteristics observed in individuals from quake-damaged regions and summarizes the strengths and functionality of imaging modalities. In such circumstances, where quick decision-making processes are life-saving and essential, we hope this review will be a practical reference for readers.

KEYWORDS

Earthquakes, disasters, embolism, emergencies, crush injuries, compartment syndromes, multiple trauma, radiology information systems

Earthquakes are among the most destructive and unpredictable natural disasters.¹ A magnitude 7.7 foreshock occurred in the epicenter of the Kahramanmaraş earthquake at 04:17:35 (UTC +03:00) on February 6, 2023. Then, at 13:24:49 (UTC+03:00), another earthquake of magnitude 7.6 occurred with its epicenter in Kahramanmaraş-Elbistan (Figure 1).^{2,3} The natural calamity devastated 10 cities, and thousands of injured individuals were taken to hospitals throughout Turkey. In the first month after the earthquake, it was reported that 46,104 people had perished and over 100,000 were injured as a result of the quakes centered in Kahramanmaraş.⁴

Various diseases and ailments, such as bone fractures, organ and soft-tissue injuries, cardiovascular diseases, lung diseases, and infectious diseases, can develop in the aftermath of severe earthquakes. Digital radiography (DR), ultrasound (US), computed tomography (CT), and magnetic resonance imaging (MRI) are significant imaging modalities utilized for the quick and reliable assessment of earthquake-related ailments to facilitate the planning of suitable therapy.⁵

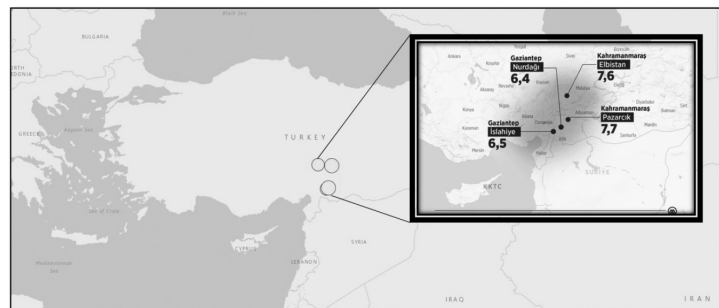


Figure 1. Epicenters and magnitudes of the recent earthquakes occurring in the south of Turkey.

Corresponding author: Omer Kazci

E-mail: omerkazci1990@gmail.com

Received 17 February 2023; revision requested 06 March 2023, accepted 03 April 2023.



Epub: 24.04.2023

Publication date: 08.01.2023

DOI: 10.4274/dir.2023.232157

You may cite this article as: Aydin S, Kazci O, Ece B, Kantarci M. Earthquakes from a radiological perspective: what is demanded from the radiologists, and what can we do? A pictorial review. *Diagn Interv Radiol.* 2024;30(1):30-41.

Based on previously published experiences after major earthquakes, this article examines the typical radiological imaging characteristics observed in individuals from quake-damaged regions and summarizes the strengths and functionality of imaging modalities. In this way, it aims to provide a practical source of information to radiologists during fieldwork in large-scale disasters where rapid diagnosis is of great importance.

Imaging method availability and utility

Ultrasound: US is the most useful and accessible method, both at the time of the disaster and in the following six-hour period. The main reason for this is the energy requirement of imaging methods. As the sole method of cross-sectional imaging accessible while CT was unavailable, US was widely utilized (it is easy to get to, can be used on the go, and helps doctors figure out which injuries are superficial and which are internal). US proved invaluable in the initial phases following the disaster, especially in the absence of CT, and should be incorporated into local disaster or mass-casualty strategies.⁶ Larger devices are less useful than portable ones. Even in the absence of biochemical laboratory tests, portable ultrasonography instruments can aid in narrowing the differential diagnosis or ruling out more serious illnesses. It is portable, simple, and painless, and in many instances, it has provided rapid results.⁷

Focused Assessment with Sonography for Trauma (FAST) is the main sonographic method for earthquake-related ailments (Figure 2). After Hurricane Katrina, 9/11 in New York, the Lebanon War in 2006, and the Iran earthquake in 2010, FAST was found to be successful in assessing and triaging patients during

periods of high patient volume. In the acute post-disaster phase, it can be utilized to check for hemothorax/pneumothorax, solid organ injury, fractures, pregnancy and vascular investigations, pediatric head scans, and intravenous access help.⁸ A clinician can perform FAST with the same sensitivity but less specificity compared to a radiology assistant. In addition, FAST can reduce the number of needless CT scans. In a study conducted after an earthquake in Christchurch, New Zealand, it was seen that the imaging method most frequently used and most accessible by physicians providing post-disaster health care was US (especially FAST).^{7,8}

Computed tomography: Power cuts and damage to health centers at the time of disasters seriously restrict the use of CT. It has been shown that the first use of CT in the delivery of health care to earthquake victims may extend to the fifth hour after the earthquake.⁶ Pan-CT examinations, if available, can guide emergency surgeries; nevertheless, in situations with a high patient volume, it is impossible and impractical to perform pan-CT on every patient. Therefore, FAST-guided CT examinations provide better and more effective results,⁸ and contrast-enhanced CT examinations should be approached with extreme caution. In circumstances that impede kidney function, such as crush syndrome caused by earthquakes, the use of contrast material may induce severe complications. Again, if contrast agent extravasation occurs in cases with compartment syndrome induced by earthquake-related traumas, the situation may worsen. However, in some special cases, such as suspected major vascular injury, dissection, or pulmonary embolism in a clinical examination, intravenous contrast agents can be administered without waiting for the results of the patient's kidney function tests.⁹

Digital radiography: The use of DR is also limited, for the same reasons as CT; however, DR can be commissioned more quickly because its energy requirement is less than CT. The fact that mobile DR devices allow bedside examinations provides great convenience, especially in cases with limited mobility. Versatile DR applications performed at the bedside are an important alternative in cases where CT cannot be reached. However, the fact that the batteries of these devices are sufficient for a finite time limits their use if there is a charging problem.⁶

Magnetic resonance imaging: Due to the possibility of quenching (quenching is the quick release of the liquid cryogen that keeps the MRI magnet in a superconducting state. If gas leaks into a room instead of leaving the building after an earthquake or other disaster, there is a chance of suffocation and freezing) MRI should not be utilized immediately following an earthquake.^{6,8}

Reporting alternatives

Serious difficulties have been experienced in accessing radiological images during disasters. For this reason, the ideal reporting method is verbal reporting if there is an opportunity to work closely with the clinician. In cases where there is no opportunity to work in close contact, written reports that provide short and concise information and that can be created quickly come to the forefront.⁶ After the recent earthquake disaster, it is satisfying that a system that allows remote, fast, and effective reporting was established very quickly (Figure 3).

Earthquake-related injuries

Traumatic injuries

Annually, earthquakes are the most lethal of all natural disasters. Between 2007 and 2017, 350,000 people died and over one

Main points

- Earthquake-induced power outages may limit the use of computed tomography and digital radiography and the risk of quenching may limit the use of magnetic resonance imaging.
- Ultrasonography, especially Focused Assessment with Sonography for Trauma, stands out as the most accessible and functional imaging method in disaster situations such as earthquakes.
- Contrast medium should be used with extreme caution due to the risk of rhabdomyolysis-related nephropathy.
- Knowing the typical features and distribution of earthquake-related injuries is important for rapid diagnosis and the detection of accompanying pathologies.

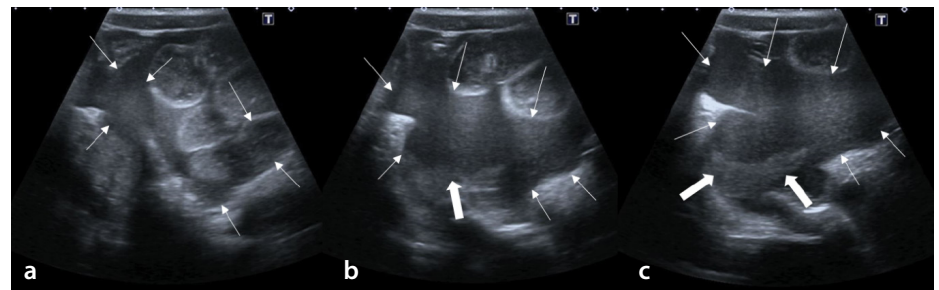


Figure 2. Intra-abdominal hemorrhage. The patient was trapped for 12 hours by earthquake debris. Eight-year-old boy, Focused Assessment with Sonography for Trauma ultrasonography images. (a) Axial view of the lower abdominal quadrant, diffuse free fluid with multiple internal echogenicities is seen between the inframezocolic bowel loops (thin arrows); (b, c) in more inferior sections, free fluid (thin arrows) with multiple internal echogenicities in the lower abdomen/pelvic region. Fluid–fluid leveling within the hemorrhage (thick arrows).

million were injured. Earthquakes appear to have a death-to-injury ratio of approximately 1:3–4,¹⁰ though this is variable depending on the severity of the injury.

In studies conducted both in our country and globally, it has been shown that the most common injuries after earthquakes are traumatic injuries, and the most needed interventions are orthopedic procedures. Debridement was the most common operation, followed by open reduction internal fixation and then closed reduction-casting.^{11–13}

Earthquake-related traumatic injuries are most common in the extremities, particularly the lower extremities. In order of frequency, extremities are followed by the thorax (Figures 4, 5), spinal injuries (Figures 6, 7), pelvic fractures, cranial and maxillofacial injuries, and abdominal traumatic findings (Figure 8).¹⁴ The femur is the most often injured bone in the extremities, followed by the tibial shaft and the ankle (Figures 9, 10). The humerus is the most often injured bone in the upper limb (Figure 11).¹⁵ It has been shown that earthquake-related lower extremity fractures, unlike other traumas, have a high rate of being multiple and comminuted (Figure 12).^{16,17} The characteristics of earthquake-related fractures seen in children are similar to adults; fractures are most commonly seen in the lower extremities, and external fixation is usually required.¹⁸

Pelvic fractures are generally seen as multiple and bilateral (Figure 13). In a study conducted in China, the most common pelvic fracture subtype was reported as type C, followed by type B3 and type B2.¹⁹ In a study conducted in Turkey, type C2 fractures were found most frequently, similar to the Chinese data (Table 1).^{20,21}



Figure 3. Workload management after the earthquake.

When the distribution of maxillofacial traumas is examined, it is seen that mandibular fractures are the most common, followed by the zygomatic complex and maxilla. Similar to lower extremity fractures, multiple and comminuted fractures are common. Cranial injuries and lower extremity fractures are the most common types of injuries to accompany maxillofacial fractures (Figure

14).^{22,23} Some studies report that nasal bone, ethmoid bone, and orbital fractures are also common. Maxillofacial fractures are injuries that require a multidisciplinary approach due to the complex anatomy of the region and the frequent occurrence of accompanying cranial traumas.²³

Additionally, one of the disorders associated with earthquakes is aggressive rhab-

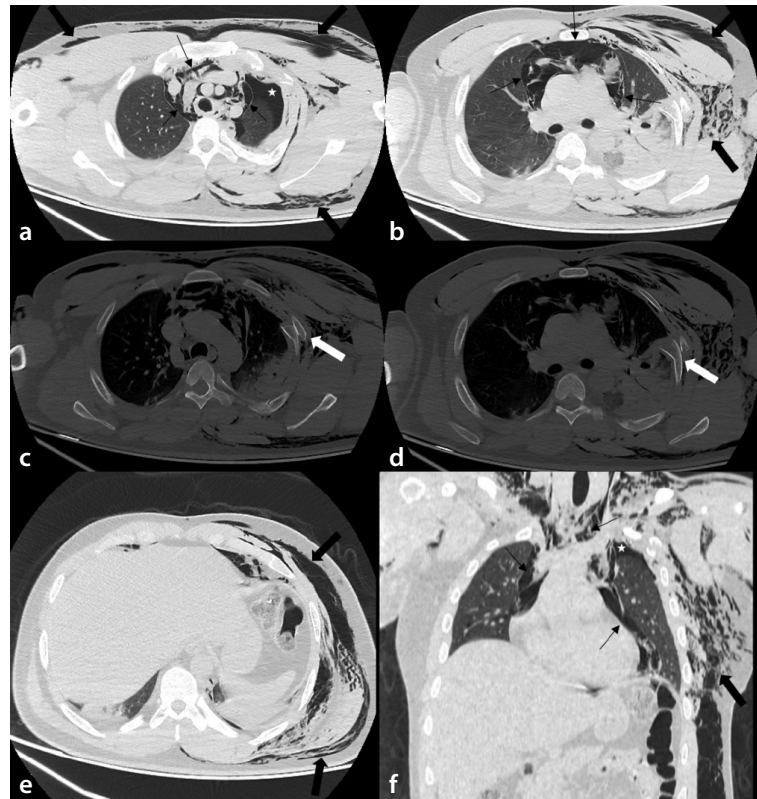


Figure 4. Traumatic pneumothorax, pneumomediastinum the patient was trapped for 19 hours by earthquake debris. Forty-three-year-old male. (a) On the axial images passing through the upper thoracic region, multiple air densities in the mediastinum (thin black arrows, pneumomediastinum), air densities near the left lung upper lobe (asterisk, pneumothorax), and diffuse subcutaneous emphysema more dominantly in the left hemithorax are seen (thick black arrows). (b) Pneumomediastinum (thin black arrows) and diffuse subcutaneous emphysema (thick black arrows) are seen in the axial sections passing through the middle part of the thorax. (c, d) Displaced rib fracture and extension of bone fragment into lung parenchyma on bone window axial section images are seen (thick white arrows). (e) Diffuse subcutaneous emphysema (thick black arrows) is seen in the axial sections passing through the inferior part of the thorax. (f) Pneumomediastinum (thin black arrows), pneumothorax (asterisk) and diffuse subcutaneous emphysema (thick black arrows) are seen in the coronal images.

Table 1. Tile classification of pelvic fractures

Type A (the pelvic ring is stable both rotationally and vertically)	A1: The fracture is observed, but the pelvic ring is not affected A2: A pelvic ring fracture is noticed, but the pelvic ring is stable
Type B (the pelvic ring is vertically stable but rotationally unstable)	B1: The appearance is likened to an open book B2: Detecting ipsilateral lateral compression B3: The contralateral or bucket handle injury pattern is examined for lateral compression.
Type C (both rotationally and vertically, the pelvic ring is unstable)	C1: Unilateral C2: Bilateral C3: Associated with acetabular fracture

domyolysis, which appears heterogeneously hypodense on CT. On post-contrast images, there may be rim enhancement. Rhabdomyolysis exhibits more diverse findings on MRI. It is also possible to detect the status of myonecrosis with MRI findings; in mild to moderate cases, damaged muscles exhibit edema, with signal intensity matching the severity of the injury. If severe myonecrosis

occurs, two different patterns can be seen: (a) homogeneously iso/hyperintense on T1 weighted images (WI), homogeneously hyperintense on T2WI/short tau inversion recovery homogeneously enhancing on postcontrast T1WI, and (b) homogeneously/heterogeneously hyperintense on T1WI, heterogeneously hyperintense on T2WI, rim-like enhancement on postcontrast T1WI

(Figure 15).²⁴ Based on data from an experimental animal study, contrast-enhanced ultrasonography (CEUS) is effective in the prehospital or bedside diagnosis of rhabdomyolysis. The study revealed that, compared with uninjured muscles, injured muscles showed early and high enhancement in CEUS images.²⁵

Acute compartment syndrome is a surgical emergency that poses limb- and life-threatening risks. It is a painful condition brought on by increased intracompartmental pressure, which compromises perfusion and causes muscle and nerve damage inside the affected compartment. The diagnosis of acute compartment syndrome is based on clinical symptoms and measurements of compartmental pressures. Utilization of imaging techniques is often restricted, and in some instances, imaging can delay diagnosis and surgical therapy. In addition to the aforementioned signs of rhabdomyolysis, MRI reveals herniation of muscle through a tear in the surrounding fascia. In addition, CT angiography and color Doppler US can be utilized to detect vascular luminal constriction due to elevated intracompartmental pressure (Figure 16).^{26,27}

Non-traumatic injuries

Cerebrovascular diseases: The increase in blood pressure and heart rate caused by the activation of the sympathetic nervous system in those impacted by a natural disaster is known as "disaster hypertension".²⁸ Hypertension is connected with an increased risk of stroke (Figure 17) and heart attack and is one of the primary causes of cardiovascular disease. In addition, various challenges connected with evacuee life (such as poor diet and water, difficulty obtaining regular medicine, and mental stress) may have a negative impact on disaster hypertension, resulting in cerebrovascular strokes and cardiovascular disorders. It was known that several of the patients in the evacuation facilities had suffered cerebrovascular attacks.²⁹ One month after an earthquake, spinal subdural and epidural hematomas that were not caused by trauma were also observed. It has been claimed that irregular use of antiplatelet medications and/or an uncomfortable posture resulting from spending nights in certain vehicles are potential risk factors for these types of hematomas.⁵

Cardiovascular diseases: Heart failure (HF), lower-extremity deep vein thrombosis (DVT), and pulmonary thromboembolism (PTE) are among the leading non-traumatic

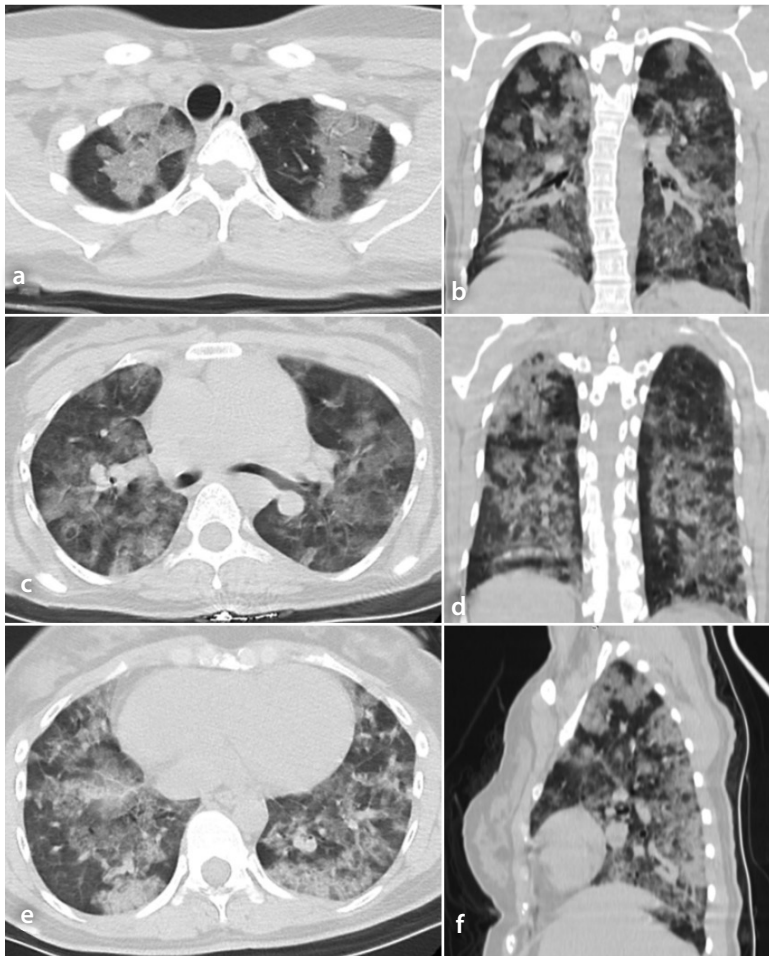


Figure 5. Diffuse alveolar hemorrhage. The patient was trapped for 22 hours by earthquake debris. Forty-three-year-old male. Diffuse widespread ground glass opacities and consolidations. (a, c, e) Axial images from different levels; (b, d) coronal images from different levels; (f) sagittal.



Figure 6. Type 2 odontoid fracture. The patient was trapped for 9 hours by earthquake debris. Thirty-nine-year-old male. A fragmented and displaced fracture of the odontoid process (arrows) is seen on axial (a) and coronal (b) computed tomography images.

diseases associated with earthquakes (Figures 18, 19).^{30,31} While HF increases occur over long periods, such as into the seventh week

after the earthquake, PTE and DVT cases increase closer to the occurrence of the earthquake. In addition, DVT and PTE more com-

monly affect women; it is thought that the primary reason for this is the combination of oral contraceptives with prolonged sitting or inadequate living conditions.^{30,31}

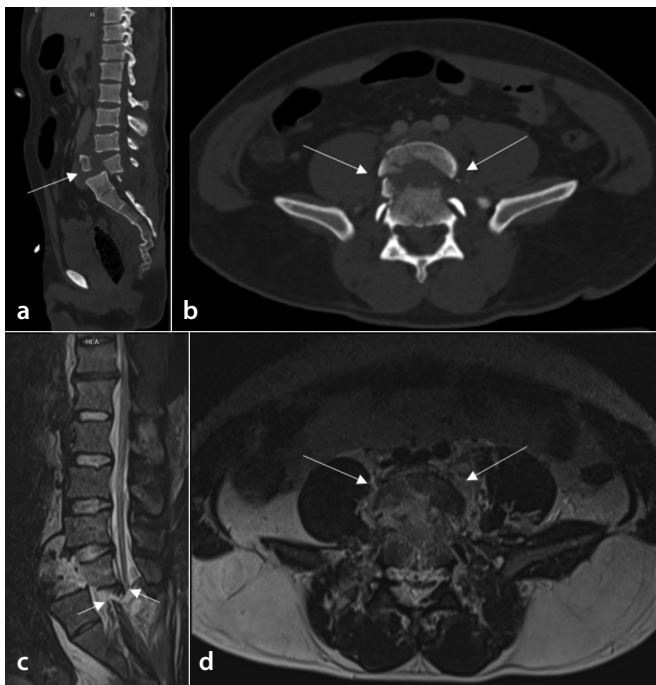


Figure 7. Traumatic listhesis and spinal cord injury. The patient was trapped for 31 hours by earthquake debris. Forty-one-year-old male. Retrolisthesis due to burst fracture of the L5 vertebrae (arrows) on the L5-S1 level. Spinal cord transection is seen on coronal Short tau inversion recovery (STIR) (c, arrows point to the two dissected edges of the spinal cord) (a) coronal computed tomography (CT) image, (b) axial CT image, (c) coronal STIR, (d) axial T2 weighted image.

Infections: Problems in clean water supply and sewage systems and poor housing conditions in evacuation centers are the main causes of post-disaster infections. Respiratory and gastrointestinal infections constitute the most common group, and increased cases of meningoencephalitis have also been reported after disasters (Figure 20).^{32,33} It has been shown that common orthopedic injuries are accompanied by wound infections in approximately 20% of cases.³³

Interventional radiologic procedures: In disaster situations such as earthquakes, where access to CT and fluoroscopy devices is limited, interventional radiological procedures cannot be widely performed. However, it is seen that the procedures performed under US guidance are practical and life-saving. Tube thoracotomies, pleural hemorrhage drainage, and central venous catheter procedures are the main life-saving interventional radiology applications in disaster areas.³⁴

Injuries with high mortality risk and forensic medicine–radiology cooperation

Immediate deaths are those that result from catastrophic injuries sustained during the earthquake. Severe trauma to the brain or spinal cord is a common cause of such injuries, and in most cases, these patients cannot be saved. Other earthquake victims die rapidly within the first few hours following the catastrophe, and historical experience indicates that mortality could be drastically decreased if treatment is administered promptly. These people suffer subdural hematomas, lacerations to the liver or spleen, and pelvic fractures. The third peak of mortality, which comes days to weeks following the earthquake, is caused by sepsis, multi-system organ failure, and disseminated intravascular coagulation. These individuals have the highest possibility of being saved since they succumb to injury complications more slowly.³⁵

Unfortunately, one of the post-disaster medical efforts is to determine the identities of those who lost their lives. At this point, forensic medicine physicians can also apply imaging methods. Considering the possibilities that the disaster environment can offer, it has been determined that the most frequently used method is dental radiographs. It is known that MRI and CT are highly functional in determining and clarifying the



Figure 8. Different patterns of traumatic abdominal injury. The patient was trapped for 35 hours by earthquake debris. Forty-seven-year-old male (a) American Association for the Surgery of Trauma (AAST) grade III injury in the right lobe-segment VII. (b) Left surrenal hematoma (circle), large perisplenic hematoma (arrows), splenic arterial injury, and corresponding contrast medium extravasation (thick arrow) (AAST grade V injury). (c) Large perisplenic hematoma (arrows), splenic arterial injury, and corresponding contrast medium extravasation (thick arrow). Sudden luminal narrowing in the left renal artery (circle) observed secondarily to blunt trauma. (d) Renal parenchymal infarct (arrows) due to the arterial narrowing shown in d (AAST grade V injury).

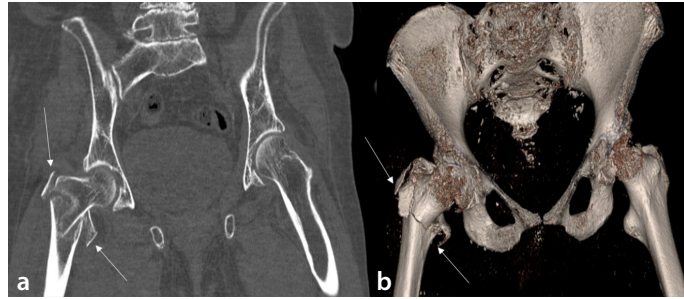


Figure 9. Intertrochanteric femur fracture. It was not possible to determine how long the patient was trapped by earthquake debris. Thirty-eight-year-old male. Displaced and comminuted fracture (arrows) in the right femoral intertrochanteric region on the coronal (a) and three-dimensional reconstruction (b) computed tomography images.

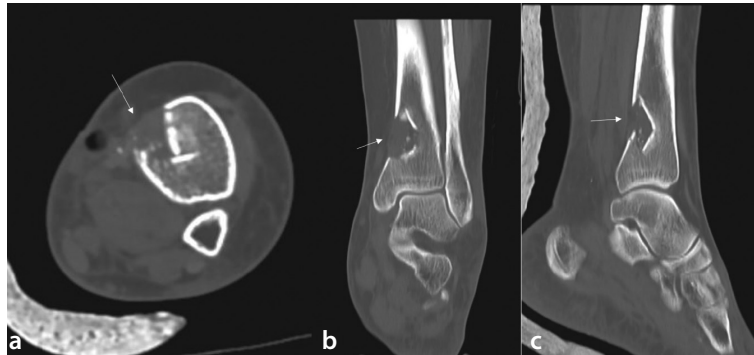


Figure 10. Distal tibial fracture. It was not possible to determine how long the patient was trapped by earthquake debris. Thirty-year-old male. (a) Medial cortical depression and internal displaced fracture (arrow) are seen in the distal metaphyseal–diaphyseal part of the tibia on axial (a), coronal (b), and sagittal (c) computed tomography images.

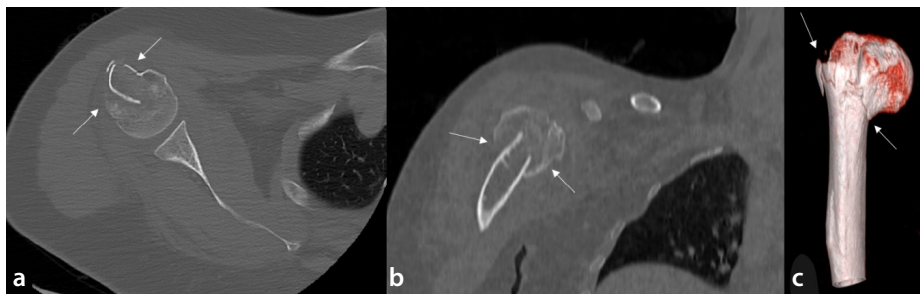


Figure 11. Proximal humeral fracture. It was not possible to determine how long the patient was trapped by earthquake debris. Sixty-year-old female. Fracture is seen in the surgical neck of humerus fracture (arrows) (a: axial view, b: coronal view, c: three-dimensional image).



Figure 12. Multiple lower extremity fractures. The patient was trapped for 23 hours by earthquake debris. Thirty-three-year-old male. Minimally displaced fractures are present in the medial malleolus of the tibia and distal metaphysis of the fibula on X-ray (a), coronal computed tomography (b), and three-dimensional reconstruction (c) images.



Figure 13. Pelvic and humeral fractures. The patient was trapped for 29 hours by earthquake debris. Seventy-six-year-old male. Displaced and comminuted fractures are seen in the left acetabulum and femoral neck (thin arrows) on axial (a) and coronal (c) computed tomography (CT) images. Large intramuscular hematoma due to the fractures is present on axial CT image (b, thick arrow). The fractures extend towards the iliac wing and inferior pubic ramus on the three-dimensional reconstruction image (d, arrow, Tile type A2 fracture).

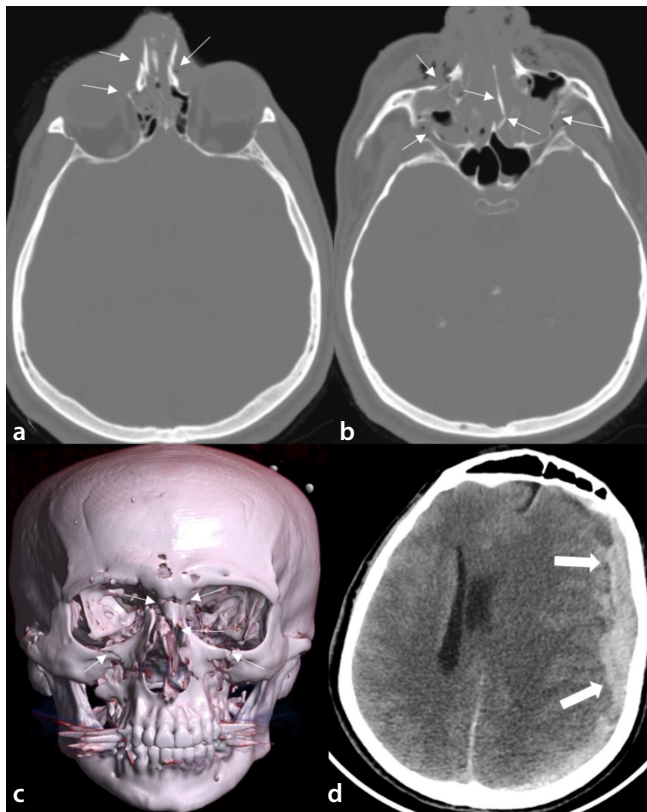


Figure 14. Multiple maxillofacial fractures and accompanying cranial hemorrhage. The patient was trapped for 17 hours by earthquake debris. Forty-four-year-old male. Multiple displaced fractures (thin arrows) are seen in maxillofacial bones in axial (a, b) and 3D reconstruction (c) computed tomography images. Extensive subdural hemorrhage causing a shift in midline structures accompanies the fractures (d, thick arrows).

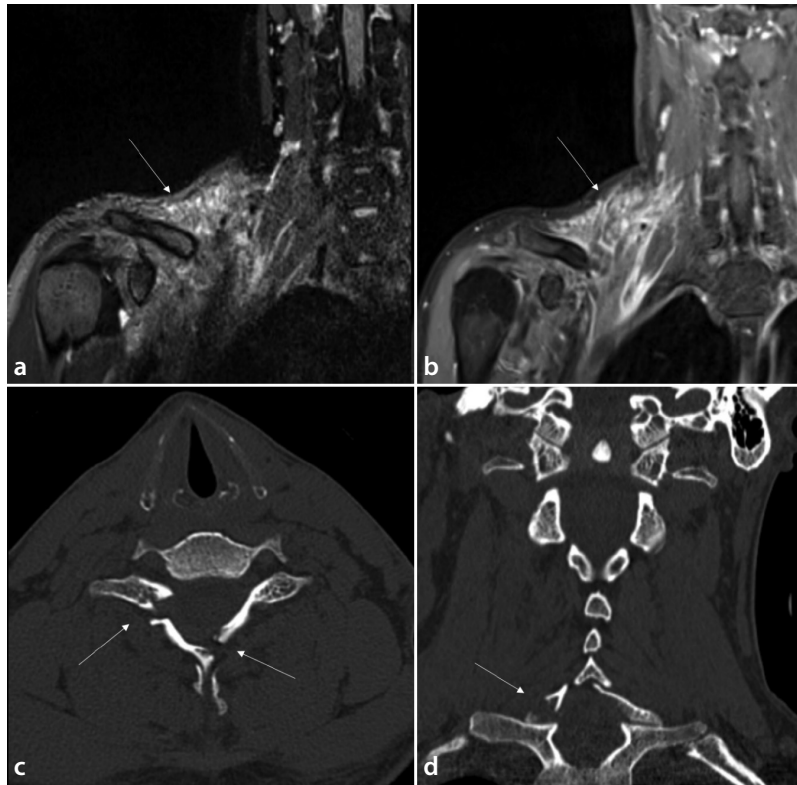


Figure 15. Rhabdomyolysis. The patient was trapped for 39 hours by earthquake debris. Twenty-year-old male. Rhabdomyolysis due to brachial plexus damage secondary to cervical fracture. Rhabdomyolysis (arrows) is seen as hyperintense on short tau inversion recovery (a) and it enhances on post-contrast T1 weighted image (b). The displaced fracture in the bilateral arch of the C7 vertebrae (arrows) is seen in axial (c) and coronal (d) sections on computed tomography.

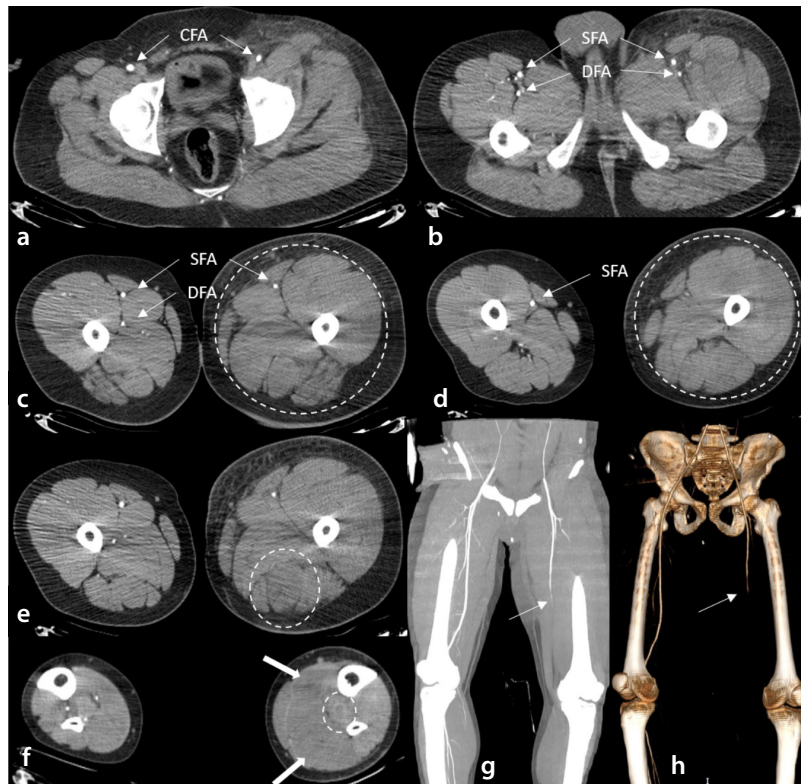


Figure 16. Compartment syndrome and rhabdomyolysis. The patient was trapped for 51 hours by earthquake debris. Thirty-four-year-old male. Left lower extremity is larger and subcutaneous edema is present (a-e). Common femoral artery, superficial femoral artery (SFA), and deep femoral artery are normal in the proximal segments of the left lower extremity (a-c). Due to increased intracompartmental pressure, left SFA narrows suddenly (d, g, h, arrows). Semitendinosus (e, circle) and gastrocnemius (f, arrows) muscles are hypodense; there is a ring-enhancing lesion in the popliteus muscle (f, circle) due to rhabdomyolysis.

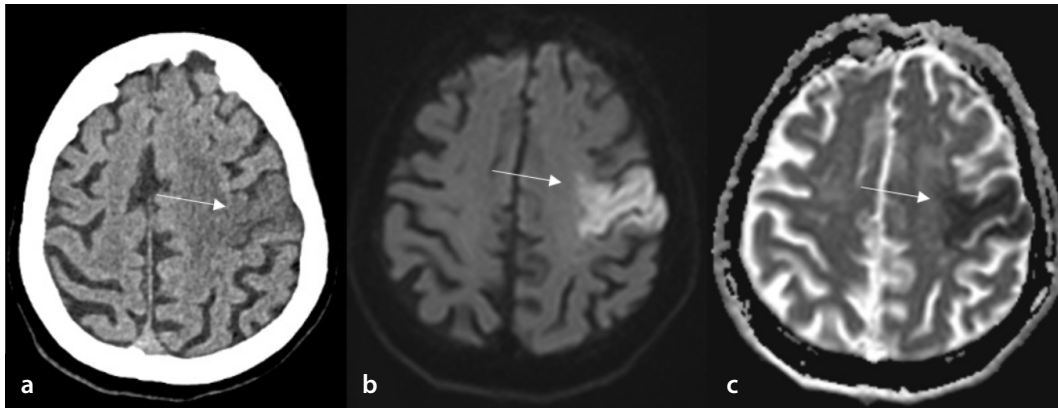


Figure 17. Acute cerebral infarction. Forty-four-year-old male, diagnosed 50 hours after being rescued from rubble. Ischemic brain parenchyma is seen as a hypodense area on computed tomography (a); corresponding diffusion restriction can be seen on diffusion-weighted imaging (b) and apparent diffusion coefficient map (c).

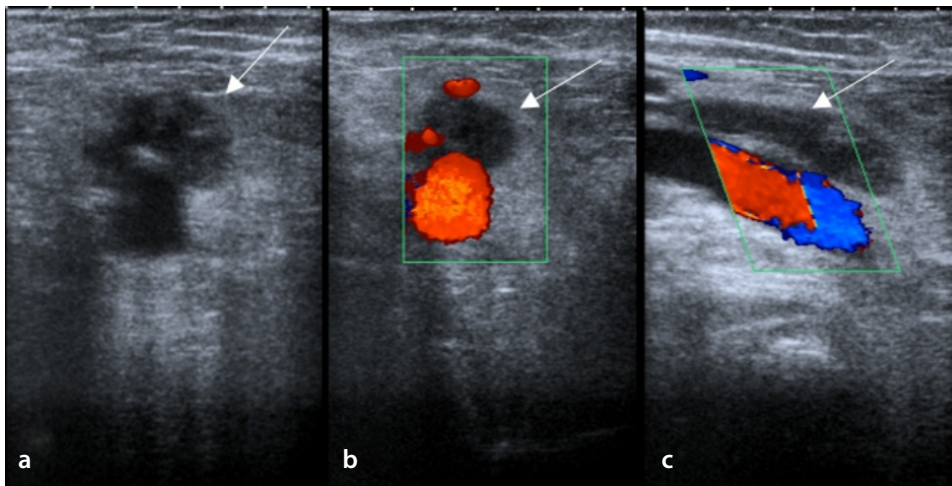


Figure 18. Deep vein thrombosis. Fifty-three-year-old female, diagnosed after rescue after 13 hours in the rubble. Thrombosis is seen in the superficial femoral vein (arrows) on grayscale ultrasound (a), axial (b), and longitudinal color Doppler ultrasonography images (c).

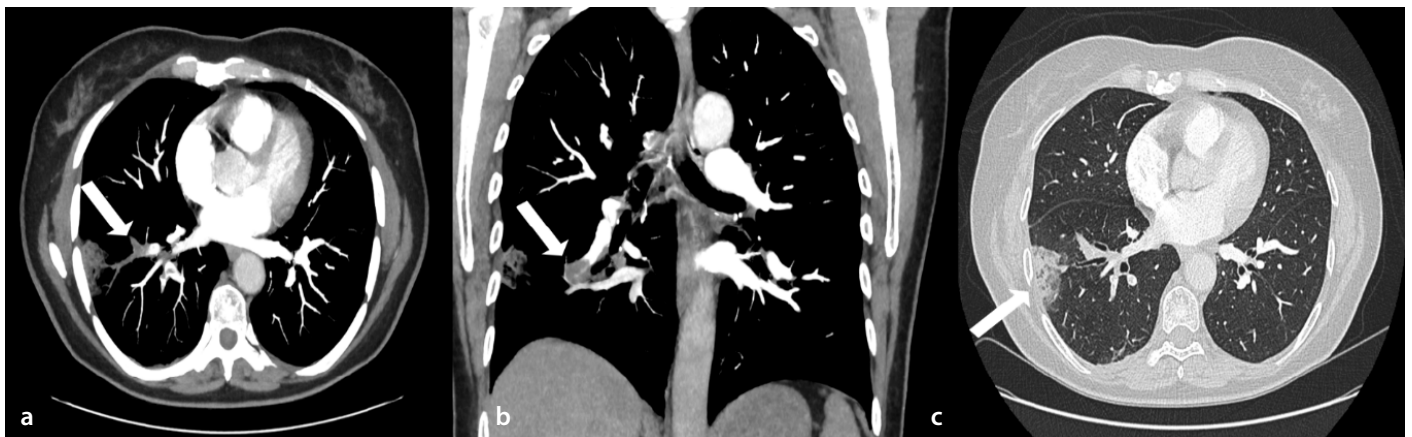


Figure 19. Pulmonary thromboembolism (PTE). The patient was trapped for 41 hours by earthquake debris. Forty-seven-year-old female. Filling defect corresponding to PTE, detected after 72 hours from the rescue from a rubble, is seen on axial (a, arrow) and coronal (b, arrow) images. A peripheral lung necrosis due to PTE is seen on the axial image with parenchymal windowing (c, arrow).

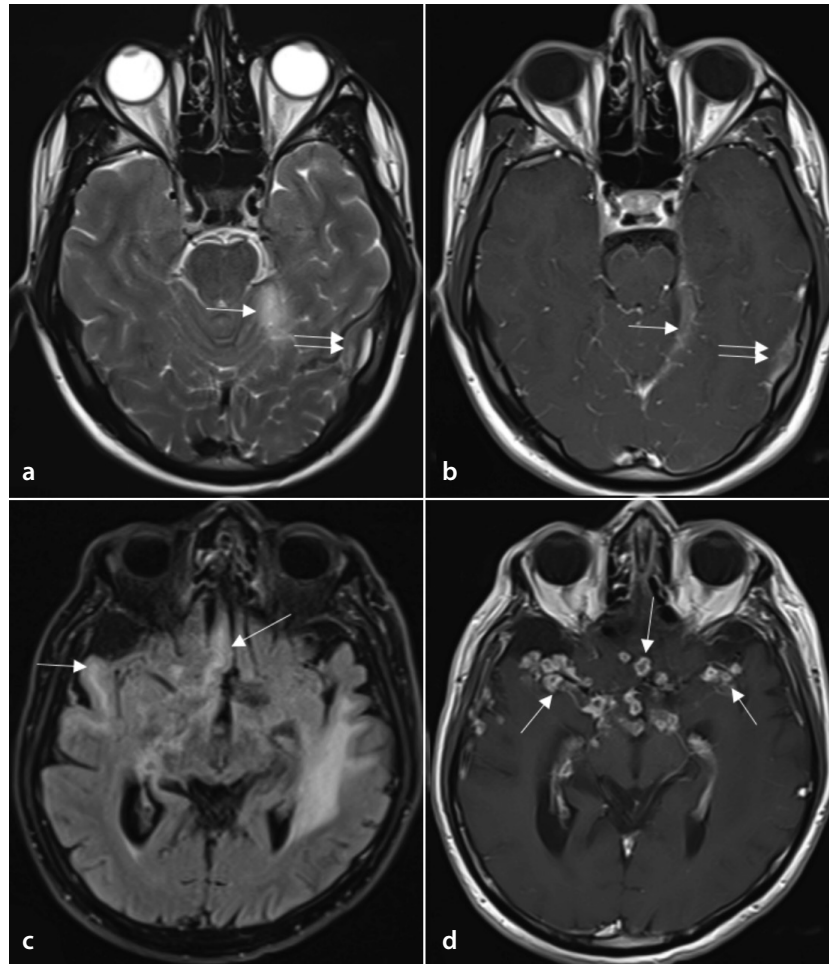


Figure 20. Viral meningitis (**a, b**) and tuberculous meningitis (**c, d**). Forty-three-year-old female and 73-year-old male, respectively. The images were obtained after 53 and 83 hours in the rubble, respectively.

Viral meningitis: left tentorium cerebelli is seen thickened and hyperintense on T2 weighted image (WI) (**a**, arrow), left temporal lobe and neighboring dura is hyperintense on T2WI (**a**, double arrow) (**a**), increased contrast enhancement is present in both corresponding areas (**b**).

Tuberculous meningitis: faint hyperintensities are present in the bilateral basal areas of the temporal lobes on fluid attenuated inversion recovery (**c**, arrows); increased contrast enhancement and ring-enhancing lesions can be seen in both corresponding areas (**d**, arrows).

cause of death, but, unfortunately, the use of both methods is limited. The main reasons for this are the great need for life-saving interventions for these imaging methods and the large number of bodies that need to be examined in an environment where there is mass loss of life. In addition, it has been observed that many radiologists do not have enough experience in forensic imaging.^{36,37}

In conclusion, in earthquakes and similar disaster situations, the need for imaging methods increases, and imaging plays an important role in saving lives. Due to the constraints in energy supply and easy accessibility, US examinations—especially FAST—have become the most useful method. Knowing the most common injuries, typical imaging findings of these injuries and their accompanying pathologies will help save more lives. Reporting procedures in close contact with the clinician, verbally or in the form of short notes, seems to be the most useful method. It should not be forgotten that the establishment of remote reporting systems is a practical and effective solution in cases where there is excessive demand.

Conflict of interest disclosure

Sonay Aydın, MD, is Section Editor in Diagnostic and Interventional Radiology. He had no involvement in the peer-review of this article and had no access to information regarding its peer-review. Other authors have nothing to disclose.

References

- Ishihara O, Yoshimura Y. Damages at Japanese assisted reproductive technology clinics by the Great Eastern Japan Earthquake of 2011. *Fertil Steril*. 2011;95(8):2568-2570. [\[CrossRef\]](#)
- United States Geological Survey (USGS), Earthquakes maps, Accessed February 15, 2023. [\[CrossRef\]](#)
- Anadolu Agency Infographics, Accessed February 15, 2023. [\[CrossRef\]](#)
- Earthquake news, Accessed March 8, 2023. [\[CrossRef\]](#)
- Iyama A, Utsunomiya D, Uetani H, et al. Emergency radiology after a massive earthquake: clinical perspective. *Jpn J Radiol*. 2018;36(11):641-648. [\[CrossRef\]](#)
- Gregan J, Balasingam A, Butler A. Radiology in the Christchurch earthquake of 22 February 2011: challenges, interim processes and clinical priorities. *J Med Imaging Radiat Oncol*. 2016;60(2):172-181. [\[CrossRef\]](#)
- Raja FS. Portable sonography in Haiti after the earthquake. *Can Assoc Radiol J*. 2011;62(3):222. [\[CrossRef\]](#)
- Kakaei F, Zarrintan S, Rikhtegar R, Yaghoobi AR. Iranian 2012 earthquake: the importance of Focused Assessment with Sonography for Trauma (FAST) in assessing a huge mass of injured people. *Emerg Radiol*. 2013;20(4):307-308. [\[CrossRef\]](#)
- Stavarakakis IM, Daskalakis II, Detsis EPS, Karagianni CA, Papantonaki SN, Katsafarou MS. Hand compartment syndrome as a result of intravenous contrast extravasation. *Oxf Med Case Reports*. 2018;2018(12):omy098. [\[CrossRef\]](#)
- Bartholdson S, von Schreeb J. Natural disasters and injuries: what does a surgeon need to know? *Curr Trauma Rep*. 2018;4(2):103-108. [\[CrossRef\]](#)
- Dursun R, Görmeli CA, Görmeli G. Evaluation of the patients in Van Training and Research Hospital following the 2011 Van earthquake in Turkey. *Ulus Travma Acil Cerrahi Derg*. 2012;18(3):260-264. [\[CrossRef\]](#)
- Guner S, Guner SI, Isik Y, et al. Review of Van earthquakes from an orthopaedic perspective: a multicentre retrospective study. *Int Orthop*. 2013;37(1):119-124. [\[CrossRef\]](#)
- MacKenzie JS, Banskota B, Sirisreerux N, Shafiq B, Hasenboehler EA. A review of the epidemiology and treatment of orthopaedic injuries after earthquakes in developing countries. *World J Emerg Surg*. 2017;12:9. [\[CrossRef\]](#)
- Dong ZH, Yang ZG, Chu ZG, et al. Earthquake-related injuries: evaluation with multidetector computed tomography and digital radiography of 1491 patients. *J Crit Care*. 2012;27(1):103.e1-103.e6. [\[CrossRef\]](#)
- Blumberg N, Lebel E, Merin O, Levy G, Bar-On E. Skeletal injuries sustained during the Haiti earthquake of 2010: a radiographic analysis of the casualties admitted to the Israel Defense Forces field hospital. *Eur J Trauma Emerg Surg*. 2013;39(2):117-122. [\[CrossRef\]](#)
- Chen TW, Yang ZG, Dong ZH, et al. Earthquake-related crush fractures and non-earthquake-related fractures of the extremities: a comparative radiological study. *Emerg Med Australas*. 2012;24(6):663-669. [\[CrossRef\]](#)
- Chen TW, Yang ZG, Wang QL, et al. Crush extremity fractures associated with the 2008 Sichuan earthquake: anatomic sites, numbers and statuses evaluated with digital radiography and multidetector computed tomography. *Skeletal Radiol*. 2009;38(11):1089-1097. [\[CrossRef\]](#)
- Morelli I, Sabbadini MG, Bortolin M. Orthopedic injuries and their treatment in children during earthquakes: a systematic review. *Prehosp Disaster Med*. 2015;30(5):478-485. [\[CrossRef\]](#)
- Chen TW, Yang ZG, Dong ZH, Chu ZG, Yao J, Wang QL. Pelvic crush fractures in survivors of the Sichuan earthquake evaluated by digital radiography and multidetector computed tomography. *Skeletal Radiol*. 2010;39(11):1117-1122. [\[CrossRef\]](#)
- Görmeli CA, Görmeli G, Güner S, et al. Evaluation of pelvic fractures by radiographical and multi-detector computed tomography following the 2011 Van earthquake in Turkey. *Eastern Journal of Medicine*. 2014;19(1):8-12. [\[CrossRef\]](#)
- Zingg T, Uldry E, Omoumi P, et al. Interobserver reliability of the Tile classification system for pelvic fractures among radiologists and surgeons. *Eur Radiol*. 2021;31(3):1517-1525. [\[CrossRef\]](#)
- Tang YL, Zhu GQ, Zhou H, et al. Analysis of 46 maxillofacial fracture victims in the 2008 Wenchuan, China earthquake. *Oral Surg Oral Med Oral Pathol Oral Radiol Endod*. 2009;108(5):673-678. [\[CrossRef\]](#)
- Chu ZG, Yang ZG, Dong ZH, et al. Features of cranio-maxillofacial trauma in the massive Sichuan earthquake: analysis of 221 cases with multi-detector row CT. *J Craniomaxillofac Surg*. 2011;39(7):503-508. [\[CrossRef\]](#)
- Lu CH, Tsang YM, Yu CW, Wu MZ, Hsu CY, Shih TT. Rhabdomyolysis: magnetic resonance imaging and computed tomography findings. *J Comput Assist Tomogr*. 2007;31(3):368-374. [\[CrossRef\]](#)
- Zhang CD, Lv FQ, Li QY, et al. Application of contrast-enhanced ultrasonography in the diagnosis of skeletal muscle crush injury in rabbits. *Br J Radiol*. 2014;87(1041):20140421. [\[CrossRef\]](#)
- Mahmoud OA, Mahmoud MZ. Spectral Doppler findings in a rare case of acute compartment syndrome following leg burn. *Radiol Case Rep*. 2018;13(2):352-355. [\[CrossRef\]](#)
- Nico MAC, Carneiro BC, Zorzenoni FO, Ormond Filho AG, Guimarães JB. The role of magnetic resonance in the diagnosis of chronic exertional compartment syndrome. *Rev Bras Ortop (Sao Paulo)*. 2020;55(6):673-680. [\[CrossRef\]](#)
- Kario K. Disaster hypertension—its characteristics, mechanism, and management. *Circ J*. 2012;76(3):553-562. [\[CrossRef\]](#)
- Omama S, Yoshida Y, Ogasawara K, et al. Influence of the great East Japan earthquake and tsunami 2011 on occurrence of cerebrovascular diseases in Iwate, Japan. *Stroke*. 2013;44(6):1518-1524. [\[CrossRef\]](#)
- Aoki T, Takahashi J, Fukumoto Y, et al. Effect of the Great East Japan earthquake on cardiovascular diseases—report from the 10 hospitals in the disaster area. *Circ J*. 2013;77(2):490-493. [\[CrossRef\]](#)
- Sueta D, Akahoshi R, Okamura Y, et al. Venous Thromboembolism due to oral contraceptive intake and spending nights in a vehicle—a case from the 2016 Kumamoto Earthquakes. *Intern Med*. 2017;56(4):409-412. [\[CrossRef\]](#)
- Kouadio IK, Aljunied S, Kamigaki T, Hammad K, Oshitani H. Infectious diseases following

- natural disasters: prevention and control measures. *Expert Rev Anti Infect Ther.* 2012;10(1):95-104. [\[CrossRef\]](#)
33. Phalkey R, Reinhardt JD, Marx M. Injury epidemiology after the 2001 Gujarat earthquake in India: a retrospective analysis of injuries treated at a rural hospital in the Kutch district immediately after the disaster. *Glob Health Action.* 2011;4:7196. [\[CrossRef\]](#)
34. Ferrara S. Radiology afloat: The impact of diagnostic and interventional radiology during the 2005 tsunami relief effort aboard the USNS Mercy. *J Vasc Interv Radiol.* 2009;20(3):289-302. [\[CrossRef\]](#)
35. Bartels SA, VanRooyen MJ. Medical complications associated with earthquakes. *Lancet.* 2012;379(9817):748-757. Erratum in: *Lancet.* 2012;379(9817):712. [\[CrossRef\]](#)
36. Guglielmi G, Sica G, Palumbo L, et al. Lethal injuries following building collapse: comparison between autopsy and radiographic findings. *Radiol Med.* 2011;116(6):969-981. [\[CrossRef\]](#)
37. Lino M, Aoki Y. The use of radiology in the Japanese tsunami DVI process. *Journal of Forensic Radiology and Imaging.* 2016;4:20-26. [\[CrossRef\]](#)